MolecularMedicine

Erythropoietin Attenuates Neurological and Histological Consequences of Toxic Demyelination in Mice

Nora Hagemeyer,[1] Susann Boretius,[2] Christoph Ott,[1] Axel von Streitberg,[1] Henrike Welpinghus,[1] Swetlana Sperling,[1] Jens Frahm,[2] Mikael Simons,[3,4] Pietro Ghezzi,[5] and Hannelore Ehrenreich[1]

[1]Division of Clinical Neuroscience, Max Planck Institute of Experimental Medicine, Göttingen, Germany; [2]Biomedizinische NMR Forschungs GmbH, Max Planck Institute for Biophysical Chemistry, Göttingen, Germany; [3]Max Planck Institute of Experimental Medicine, Göttingen, Germany; [4]Department of Neurology, University of Göttingen, Göttingen, Germany; and [5]Division of Clinical and Laboratory Investigation, Brighton & Sussex Medical School, Brighton, UK

Erythropoietin (EPO) reduces symptoms of experimental autoimmune encephalomyelitis in rodents and shows neuroregenerative effects in chronic progressive multiple sclerosis. The mechanisms of action of EPO in these conditions with shared immunological etiology are still unclear. Therefore, we used a model of toxic demyelination allowing exclusion of T cell–mediated inflammation. In a double-blind (for food/injections), placebo-controlled, longitudinal four-arm design, 8-wk-old C57BL/6 mice (n = 26/group) were assigned to cuprizone-containing (0.2%) or regular food (ground chow) for 6 wks. After 3 wks, mice were injected every other day with placebo or EPO (5,000 IU/kg intraperitoneally) until the end of cuprizone feeding. Half of the mice were exposed to behavioral testing, magnetic resonance imaging (MRI) and histology immediately after treatment cessation, whereas the other half were allowed a 3-wk treatment-free recovery. Immediately after termination of cuprizone feeding, all toxin-exposed mice were compromised regarding vestibulomotor function/coordination, with EPO-treated animals performing better than placebo. Likewise, ventricular enlargement after cuprizone, as documented by MRI, was less pronounced upon EPO. After a 3-wk recovery, remarkable spontaneous improvement was observed in all mice with no measurable further benefit in the EPO group ("ceiling effect"). Histological analysis of the corpus callosum revealed attenuation by EPO of the cuprizone-induced increase in microglial numbers and amyloid precursor protein accumulations as a readout of inflammation and axonal degeneration. To conclude, EPO ameliorates neurological symptoms in the cuprizone model of demyelination, possibly by reduction of inflammation-associated axonal degeneration in white matter tracts. These findings underscore the value of future therapeutic strategies for multiple sclerosis based on EPO or EPO variants.

Online address: http://www.molmed.org
doi: 10.2119/molmed.2011.00457

INTRODUCTION

Multiple sclerosis (MS) is a heterogeneous inflammatory demyelinating disease of the central nervous system and the most common cause of neurological disability in young adults (1,2). Essentially all treatments, established or in development, focus on immunological targets to modify disease course and reduce relapse rates (3). In contrast, recombinant human erythropoietin (EPO) and EPO variants may provide a neuroprotective/neuroregenerative treatment strategy for MS (reviewed in [4]).

In fact, several preclinical studies of experimental autoimmune encephalomyelitis (EAE), the most commonly used animal model for MS, showed that EPO delayed disease onset, reduced neurological scores, improved electrophysiological and histological readouts and attenuated inflammatory cytokine production (5–16; reviewed in [4] and [17]). A first small exploratory open-label study in MS included patients with primary or secondary chronic progressive disease. These MS patients were treated with either high-dose (48,000 IU intravenously) or low-dose (8,000 IU intravenously) EPO, and safety issues and potential efficacy were evaluated (18). High-dose EPO treatment was well tolerated and resulted in improvement of motor and cognitive performance. Interestingly, this beneficial effect persisted for as long as up to 6 months after cessation of EPO infusions (18).

High-dose peripherally applied EPO was shown in humans and mouse to penetrate an intact blood-brain barrier in an amount sufficient to achieve neuroprotective effects in the brain (17,19). The mechanisms of action of EPO underlying

Address correspondence to *Hannelore Ehrenreich, Max Planck Institute of Experimental Medicine, Hermann-Rein-Str. 3, 37075 Göttingen, Germany. Phone: +49-551-3899-628; Fax: +49-551-3899-670; E-mail: ehrenreich@em.mpg.de.*
Submitted November 25, 2011; Accepted for publication February 28, 2012; Epub (www.molmed.org) ahead of print February 29, 2012.

The Feinstein Institute for Medical Research North Shore LIJ

its neuroprotective/neuroregenerative properties in EAE and MS, which share an immunological etiology, are still subject to speculation and may involve anti-inflammatory, antiapoptotic, antioxidative and neurotrophic effects (reviewed in [17] and [20]).

We wondered whether EPO would also show neuroprotection in an etiologically different situation of even more pronounced demyelination. Hence, we used the copper chelator cuprizone, which leads to almost complete demyelination of the corpus callosum. This model permits focusing on demyelination without interfering T cell–mediated immune-inflammatory components. Considering the seemingly beneficial effects of EPO in chronic progressive MS where acute immune-inflammatory processes are replaced by smoldering progression, we hypothesized that EPO treatment would also alleviate the cuprizone-induced changes of neurological, imaging and histological readouts.

MATERIALS AND METHODS

Animals

All experiments were approved by and conducted in accordance with the regulations of the local animal care and use committee (Niedersächsisches Landesamt für Verbraucherschutz und Lebensmittelsicherheit; AZ 33.11.42502-04-040/08). For all experiments, male C57BL/6 mice were used. They were housed in groups of five in standard plastic cages and maintained in a temperature-controlled environment (21 ± 2°C) on a 12-h light/dark cycle with food and water available ad libitum. During experiments, body weight was monitored twice weekly.

Experimental Design

In a double-blind (for food and injections), placebo-controlled longitudinal four-arm design, 8-wk old male C57BL/6 mice (n = 26 per group) were started on cuprizone-containing (0.2%; Sigma-Aldrich, Taufkirchen, Germany) or regular food (standard ground chow) for a total of 6 wks. After 3 wks, mice were injected every other day (11 injections in total) with placebo (solvent control) or EPO (5,000 IU/kg body weight intraperitoneally; NeoRecormon, Roche, Basel, Switzerland) up to the end of cuprizone feeding (compare Figure 1A). Half of the mice were exposed to behavioral testing, MRI and histology immediately after cessation of treatment, whereas the other half were allowed a 3-wk treatment-free recovery period before behavioral testing and MRI.

It should be noted that preliminary experiments performed with cuprizone-containing pellets instead of ground chow failed to result in any demyelination, although toxicological analysis of the pellets had proven that cuprizone was intact and active. This result may be due to the necessity of a parallel intake of cuprizone as fine powder via skin, airways and gut for producing demyelination.

Behavioral Testing

Group size in all behavioral experiments amounted to n = 13–26.

Rotarod. Rotarod is a relatively crude test for motor function, gross coordination and motor learning and consists of a rotating drum (Med Associates Inc., St. Albans, VT, USA) that is accelerated from 4 to 40 revolutions per minute over the course of 5 min. Each mouse is placed individually on the drum and the latency of falling down from the drum is recorded. To assess motor learning, the rotarod test is repeated 24 and 48 h later.

Beam balance. Beam balance is a sensitive test for (fine) motor coordination (balance) and vestibulomotor function. On the first day, two habituation phases are conducted where mice are placed on an elevated horizontal beam (25 mm in diameter, 59 cm in length), illuminated at the start side and with a dark little cage with bedding at the other end. With the goal to enter the little cage, mice are first placed directly in front of the cage (phase 1) and then in the middle of the beam (phase 2). On the second day, all mice are first habituated again on the 25-mm beam, this time being positioned on the illuminated start. This forces them to cross the whole beam for entering the little cage. For the following test, mice are placed on the start side of a 10-mm beam, and the time needed to pass the beam is recorded. On the third day, mice are again first put on the 25-mm beam and then switched onto an 8-mm beam for crossing-time measurement. If a mouse falls down, the test is repeated (maximally three trials/mouse). If all trials fail, a cut-off time of 60 s is used for calculations (average time in a healthy mouse amounts to <8 s). The results are calculated as duration on the beam in percentage of placebo control.

MRI Analysis

Upon completion of the behavioral analyses, six mice per group at both week 6 and 9 were studied by MRI. Animals were anesthetized by 1–1.5% isoflurane in a mixture of oxygen and ambient air and positive ventilated via endotracheal tube. A 3D Fast Low-Angle Shot (FLASH) MRI (repetition time [TR]/echo time [TE] = 14.9/3.9 ms, 45 min each) was performed at 9.4T (Bruker Biospin, Ettlingen, Germany) with 110-μm isotropic spatial resolution using a four-element phased-array surface coil (Bruker Biospin) for signal reception. Maps of T1 relaxation time were calculated from T1-weighted (flip angle 12°) and proton-density weighted datasets (flip angle 5°). In addition, magnetization transfer-weighted images were obtained by off-resonance irradiation (frequency offset 3 kHz, Gaussian pulse, duration 3.5 ms, flip angle 135°) to calculate the percent magnetization transfer ratio (%MTR). Brain volume (total brain, brain matter, hippocampi, ventricles) was determined by manual segmentation using Amira software (Visage Imaging GmbH, Berlin, Germany). In addition, multislice T2-weighted images were acquired with use of a fast-spin echo MRI sequence (TR/TE = 5,300/64 ms, 8 echoes, 26 sections) at an in-plane resolution of 80 μm and a section thickness of 300 μm (21).

Preparation of Brain Tissue

Animals were anesthetized with 0.25% tribromoethanol (Avertin; 0.125 mg/g

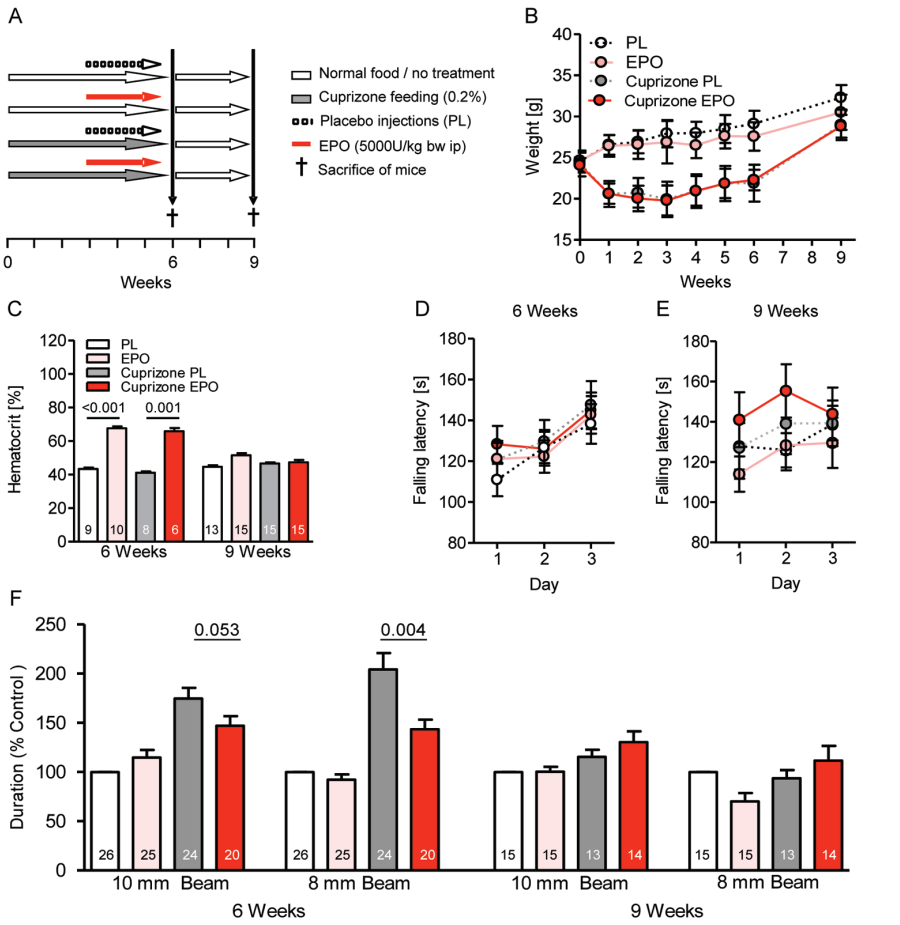

Figure 1. Clinical readouts of toxic demyelination and influence of EPO treatment. (A) Experimental design of the double-blind (for food and injections) longitudinal four-arm study. (B) Body weight curve over the experimental period shows a dramatic difference between cuprizone- and regular diet–fed mice ($P < 0.001$) but no influence of EPO (mean ± SD). (C) The hematocrit of mice is increased upon EPO at wk 6, independent of cuprizone. (D, E) Rotarod performance of mice is unaffected by cuprizone and/or EPO. (F) Beam balance performance at wk 6 is clearly compromised upon cuprizone and responds to EPO treatment. At wk 9, a remarkable recovery becomes evident. For all panels: n = 6–26 (respective n number is always given in the bar); mean ± SEM is presented.

intraperitoneally) and perfused transcardially with 0.9% saline followed by 4% paraformaldehyde. Brains were removed, fixed overnight at 4°C with 4% paraformaldehyde and placed in 30% sucrose/phosphate-buffered saline (PBS) for cryoprotection. They were frozen on liquid nitrogen. Whole mouse brains were cut into 30-µm thick coronal sections on a cryostat (Leica, Wetzlar, Germany) and kept in a storage solution (25% ethylene glycol and 25% glycerol in PBS).

Immunohistochemistry

For immunohistochemistry, serial coronal sections, spaced at regular intervals for each specific marker under investigation, were taken through the whole brain. Free floating sections were washed with PBS three times, mounted on Super Frost microscopic slides, microwaved three times in citrate buffer for 4 min and incubated with 0.5% hydrogen peroxide for 30 min to quench endogenous peroxidases. They were permeabilized and blocked for 1 h at room temperature with 5% normal serum of host species from which respective secondary antibodies were derived. Sections were incubated with mouse anti-APC (CC-1; 1:200; Merck, Darmstadt, Germany), rabbit anti-IBA1 (1:1,000; Wako, Neuss, Germany) and mouse anti-amyloid precursor protein (APP; 1:850; Millipore, Schwalbach, Germany) antibodies diluted in 3% normal serum and 0.5% Triton-X in PBS for 48 h at 4ºC. After three washes with PBS, sections were incubated with biotinylated secondary antibodies for 1.5 h. The staining was visualized by a peroxidase-labeled avidin-biotin kit (Vector Laboratories, Burlingame, CA, USA) and diaminobenzidine (Sigma-Aldrich, Taufkirchen, Germany). Sections stained for APP were counterstained with hematoxylin for 30 s. Slides were washed in PBS, air-dried overnight, put into xylol and cover-slipped using DePeX (Serva, Heidelberg, Germany).

Quantification of Cell Numbers

Digitized overlapping light microscopic images (400× oil; Zeiss, Oberkochen, Germany) from the rostral (bregma 1.10 to –0.10) and caudal (bregma –0.94 to –2.46) region of the corpus callosum (compare Figure 3A) were fused to continuous images using Photoshop CS. Cell counts were performed using ImageJ software. Cell numbers were calculated per millimeter squared. Intra- and inter-rater reliability of cell counts was conducted for all parameters and revealed highly significant correlations ($r > 0.98$; $P < 0.001$).

Isolation of Total RNA and Quantitative Real-Time Reverse Transcriptase–Polymerase Chain Reaction (RT-PCR; qPCR)

For isolation of total RNA, two coronal brain sections per mouse were used, using the RNeasy FFPE kit (Qiagen, Hilden, Germany). First-strand cDNA was generated from total RNA using N6 random primers. The relative concentrations of mRNAs of interest in different cDNA samples were measured out of

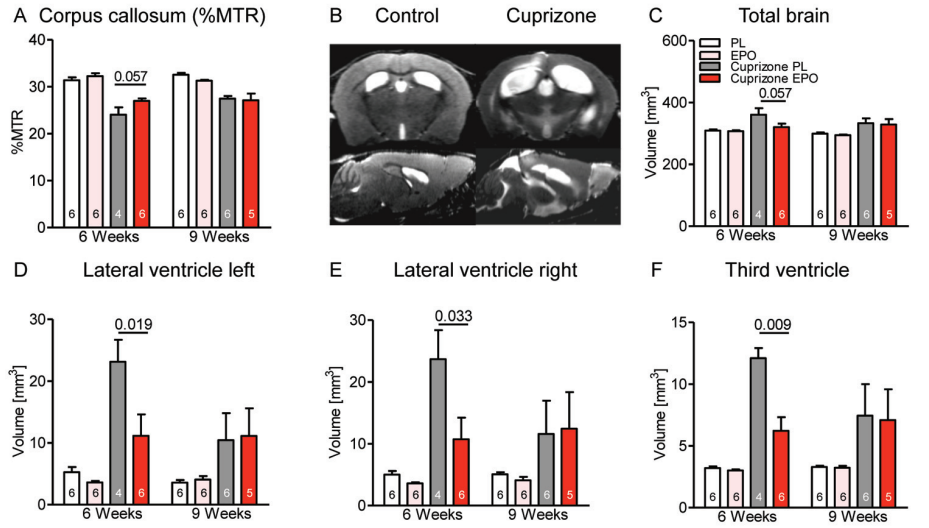

Figure 2. MRI of cuprizone-induced brain alterations and effect of EPO. (A) Presentation of the %MTR as readout of myelination in the corpus callosum after 6 wks reveals reduction by cuprizone and a trend of protection by EPO. (B) T2-weighted sample images of a control and a cuprizone-fed mouse after 6 wks illustrate brain/ventricle dimensions. Volumetrical analyses of total brain volume (C) and of ventricles (D–F) show a clear effect of EPO after 6 wks, but no longer after 9 wks. For all panels: n = 4–6 (respective n number is always given in the bar); mean ± SEM is presented.

three replicates using the threshold cycle method (delta Ct) for each dilution and were normalized to a normalization factor derived from levels of "housekeepers," glyceraldehyde-3-phosphate dehydrogenase (GAPDH), β-actin and hypoxanthine phosphoribosyltransferase 1 (HPRT1) mRNA, calculated with geNorm_win_3.5 (22). Reactions were performed using the SYBR green PCR master mix (ABgene, Foster City, CA, USA) according to the protocol of the manufacturer. Cycling was done for 2 min at 50°C, followed by denaturation at 95°C for 10 min. The amplification was carried out with 45 cycles of 95°C for 15 s and 60°C for 60 s. The specificity of each primer pair was controlled with a melting curve analysis. For qPCR, the following primers were used: mouse interleukin-1α (IL-1α) forward: 5′-TCA ACC AAA CTA TAT ATC AGG ATG TGG-3′, reverse: 5′-CGA GTA GGC ATA CAT GTC AAA TTT TAC-3′; mouse interleukin-1β (IL-1β) forward: 5′-AAG GGC TGC TTC CAA ACC TTT GAC-3′, reverse: 5′-ATA CTG CCT GCC TGA AGC TCT TGT-3′; mouse transforming growth factor-β (TGF-β) forward: 5′-TGA CGT CAC TGG AGT TGT ACG-3′, reverse: 5′-GGT TCA TGT CAT GGA TGG TGC-3′; mouse complement component 1, q subcomponent, A chain (C1qA) forward: 5′-CGG GTC TCA AAG GAG AGA GA-3′, reverse: 5′-CCT TTA AAA CCT CGG ATA CCA GT-3′; mouse triggering receptor expressed on myeloid cells-2 (Trem-2) forward: 5′-ACA GCA CCT CCA GGA ATC AAG-3′, reverse: 5′-CCA CAG CCC AGA GGA TGC-3′; mouse GAPDH forward: 5′- CAA TGA ATA CGG CTA CAG CAA C-3′, reverse: 5′-TTA CTC CTT GGA GGC CAT GT-3′; mouse β-actin forward: 5′-CTT CCT CCC TGG AGA AGA GC-3′, reverse: 5′- ATG CCA CAG GAT TCC ATA CC-3′; mouse HPRT1 forward: 5′-GCT TGC TGG TGA AAA GGA CCT CTC GAA G-3′, reverse: 5′-ATG CCC TTG ACT ATA ATG AGT ACT TCA GGG-3′.

Statistical Analysis

Data were compared using a one-tailed Mann-Whitney *U* test. Significance level was set to $P \leq 0.05$. Data are represented as mean ± standard error of the mean (SEM) unless otherwise stated. Statistical software used included Prism5 (GraphPad Software, San Diego, CA, USA) and SPSS for Windows version 17.0 (https://www.spss.com/de). (Note: The experimenters performing the experiments and data analyses were not aware of any group assignment of individual mice ["completely blinded"]).

RESULTS

Study Design and Basic Readouts Under Cuprizone and EPO

In a double-blind (for food and injections) placebo-controlled longitudinal four-arm design, 8-wk-old C57BL/6 mice (n = 26 per group) were started on cuprizone-containing (0.2%) or regular food (ground chow) for a total of 6 wks. After 3 wks, mice were injected every other day with placebo or EPO (5,000 IU/kg body weight intraperitoneally) up to the end of cuprizone feeding (study design shown in Figure 1A). Already within the first week, cuprizone led to reduced body weight of mice (monitored twice weekly), which then (independent of EPO) stayed at this lower level compared with control mice until cessation of cuprizone treatment and returned to control values thereafter (Figure 1B). Expectedly, the hematocrit increased upon EPO treatment and returned to the control range at 3 wks after termination of EPO injections (Figure 1C).

Alleviation by EPO of the Detrimental Effect of Toxic Demyelination on Vestibulomotor Coordination and Balance

Three-day rotarod tests immediately upon cessation and 3 wks after cuprizone feeding with or without EPO did not reveal any significant changes in gross motor performance and motor learning (Figures 1D, E). A more sensitive test of motor coordination and vestibulomotor function requiring interhemispheric communication is the beam balance task where mice have to cross two elevated

beams of 10 and 8 mm diameter, respectively. After 6 wks of cuprizone, mice needed significantly longer to cross the 10-mm as well as the 8-mm beam compared with untreated control mice ($P < 0.001$). EPO treatment of cuprizone mice improved performance compared with placebo (Figure 1F). After 3 wks without any treatment, all mice had reached a similar performance, underlining the pronounced spontaneous recovery after cuprizone (Figure 1F).

Mitigation of Ventricular Enlargement and Degree of Demyelination by EPO

After wk 6, the %MTR as a magnetic resonance imaging (MRI) readout correlating with myelination in the corpus callosum (23) was lower in cuprizone-treated mice, pointing to demyelination. EPO tended to counteract this decrease. After the 3-wk recovery period, there was still a decrease of %MTR compared with controls, but no measurable further benefit of EPO treatment (Figure 2A). Figure 2B illustrates typical T2-weighted brain images of a control and a cuprizone-treated animal after 6 wks. Quantification of total brain volume on the basis of high-resolution T1 maps showed an increase in cuprizone-fed mice ($P = 0.005$), an effect mitigated by EPO treatment at wk 6 (Figure 2C). This increase is explained by the known cuprizone-induced enlargement of the whole ventricular system (left and right lateral ventricle as well as third ventricle) (24), which is attenuated by EPO (Figures 2D–F). Compared to the 6-wk time point, all cuprizone-treated mice displayed a pronounced spontaneous recovery at wk 9, with no further benefit of EPO.

Attenuation by EPO of a Cuprizone-Induced Increase in Microglial Numbers and APP Accumulations as Readout of Neuroinflammation and Axonal Degeneration

To better understand the observed effects of EPO on behavioral and imaging parameters after wk 6, we chose this time point to investigate the number of oligodendrocytes and microglia as well as the degree of axonal degeneration within the corpus callosum (anatomical overview of screened regions in Figure 3A). The number of adult oligodendrocytes as stained by CC-1 (anti-APC) was remarkably reduced upon cuprizone feeding ($P < 0.001$) without any measurable benefit of EPO (Figures 3B–D). Moreover, cuprizone resulted in a significant increase in microglial numbers in the corpus callosum ($P < 0.001$), an effect diminished by EPO treatment (Figures 3E–G). In addition, axonal degeneration induced by cuprizone within the corpus callosum, as quantified by APP-positive axonal swellings, was attenuated upon EPO (Figures 3H–J). Quantitative mRNA analysis of cytokines (IL-1α, IL-1β, TGF-β) and microglia activity markers (C1qA, Trem-2) yielded a significant increase under cuprizone of the inflammation mediators IL-1α, IL-1β, C1qA and Trem-2 and a significant decrease of the protective growth factor TGF-β (all $P < 0.05$). EPO showed in several cases a tendency in the respective other direction, consistent with its counteraction of the detrimental cuprizone effects. These EPO

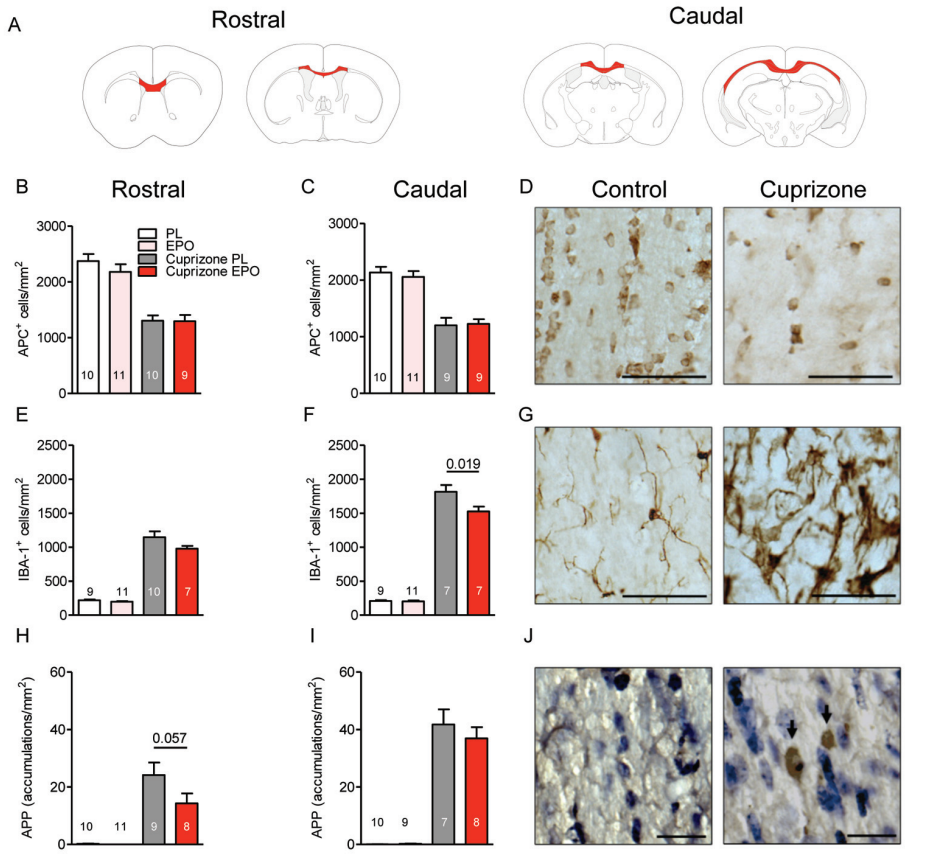

Figure 3. Cuprizone-induced changes of oligodendrocyte and microglia numbers as well as axonal degeneration in the corpus callosum: effect of EPO. All histological analyses presented have been performed after 6 wks of cuprizone ± EPO. (A) Anatomical overview of screened corpus callosum regions. (B–D) Oligodendrocytes in the rostral and caudal corpus callosum are massively reduced upon cuprizone; there was no effect of EPO (D: histological sections with scale bar 50 μm). (E–G) Microglial numbers in the rostral and caudal corpus callosum are highly increased, dampening effect of EPO (G: histological sections with scale bar 50 μm). (H–J) APP-positive accumulations in the corpus callosum (J: histological sections with accumulations indicated by arrows; scale bar 20 μm). For all panels: n = 7–11 (respective n number is always given in the bar); mean ± SEM is presented.

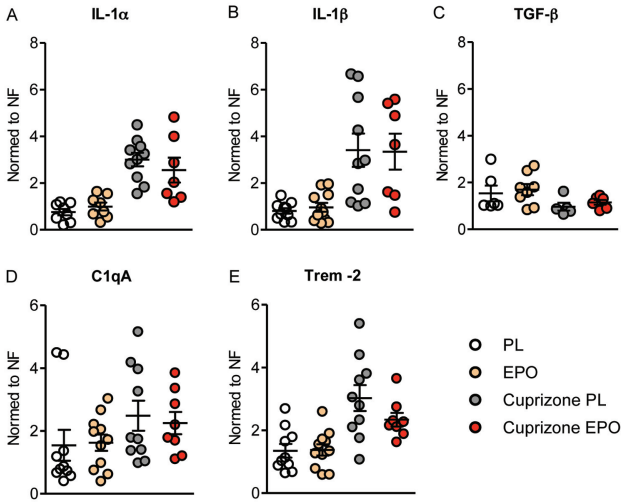

Figure 4. Cuprizone-induced alterations in brain mRNA levels of cytokines and microglia activity markers: effect of EPO. All qPCR analyses presented have been performed after 6 wks of cuprizone ± EPO. Analyses of mRNA for cytokines (IL-1α, IL-1β, TGF-β) (A–C) and microglia activity markers (C1qA, Trem-2) (D, E) yielded significant shifts under cuprizone (all $P < 0.05$). EPO showed in several cases only a slight tendency in the respective other direction (all $P > 0.05$). Expression levels are normed to the normalization factor (NF; i.e. geometric mean of GAPDH, β-actin, and HPRT1 mRNA levels). For all panels: n = 5 –11; mean ± SEM is presented. PL, placebo.

trends, however, all failed to reach statistical significance (all $P > 0.05$) (Figure 4).

DISCUSSION

This study used the cuprizone model of toxic demyelination to explore the protective potential of EPO in the absence of T cell–mediated acute immune-inflammatory processes. In this regard, the model may simulate some aspects of chronic progressive MS. Indeed, we found neurological, imaging and histological evidence for a beneficial effect of EPO in this condition.

The strong inflammatory component in this model is reflected by the highly increased numbers of microglia in the corpus callosum, associated with APP-positive accumulations as early signs of axonal degeneration. APP accumulations are likely the consequence of inflammation and are essentially absent in control mice. Both readouts of damage have been reported earlier in this model (25–28) and were found here to be reduced by EPO treatment. This reduction may at least partly explain the beneficial effects of EPO on neurological/imaging parameters (that is, vestibulomotor function and %MTR).

Attenuation by EPO treatment of microglial numbers and microglia-mediated inflammation has been demonstrated among others in models of cortical lesion (29), EAE (5,11), epilepsy (30), closed head injury (31) and ischemia (32) and has been associated with improved clinical outcome (11). In contrast, to our knowledge, reduction of APP accumulations by EPO has not been demonstrated yet. This latter finding may be secondary to EPO-mediated dampening of microglial activation and inflammation or be due to direct protective EPO effects on neurons/axons, interrupting the vicious cycle of demyelination, inflammation, compromised axonal metabolism and axonal degeneration.

Oligodendrocyte numbers were severely diminished by cuprizone but, surprisingly, no protective effects of EPO on this cell type were found here. In other models, a clear beneficial EPO effect on oligodendrocyte numbers was demonstrated (29,33). This discrepancy may be explained by the time point or brain region of cell counting selected in the present study or (more likely) by a mechanism of cell death that cannot be counteracted by EPO. Interestingly, a recent article reporting an advantageous influence of vitamin D on demyelination in the cuprizone model, strikingly similar to the results obtained here, also failed to detect effects on oligodendrocytes (34). The fact that both vitamin D and EPO act via at least one common pathway, MAPK (35), as well as seem to share mechanisms or interact regarding iron absorption or metabolism (36,37), may make future studies on a potential interplay of these agents attractive.

The beam balance test turned out to be a sensitive clinical test for measuring disability and neuroprotection by EPO in the cuprizone model. Its performance obviously requires a more sophisticated function of neuronal networks in the brain including interhemispheric communication. In contrast, the rotarod was used here as a crude motor control test, indicating simpler and more elementary functions. Not too surprising, it did not show any evidence of compromised function, an observation that had already led other authors to develop more sensitive tests for this model (38).

The cuprizone model has a number of difficulties and limitations, some of which have been mentioned in previous reports (reviewed in [26] and [39]): (a) it is variable, requiring relatively large numbers of mice for solid conclusions; (b) it is characterized by damage and recuperation running in parallel, making predictions of the right time point for measurements difficult; (c) it shows a rapid and remarkable spontaneous recovery after cessation of toxin feeding, rendering it less suitable for extended pharmacological neuroregeneration studies; and (d) last but not least, the mechanisms of damage by the copper chelator cuprizone are still incompletely characterized and subject to investigation (40). These difficulties and limitations of the cuprizone model may ultimately explain why our search for

further mechanistic insight by quantification of cytokines, known to be potently influenced by EPO and/or cuprizone in other models (41–46), or of microglial activity markers (46,47) yielded tendencies at best, but no clear-cut results.

CONCLUSION

To conclude, despite all the problems connected with the cuprizone model, there was a surprisingly clear protective effect of EPO detectable, with not all readouts reaching nominal significance but essentially all parameters adding to a mosaic: We suggest that EPO ameliorates neurological symptoms in the cuprizone model of demyelination by reduction of inflammation-associated axonal degeneration in white matter tracts. This effect of EPO may also partially explain its beneficial action in chronic progressive MS, and is worthwhile to pursue.

ACKNOWLEDGMENTS

This study was supported by the Max Planck Society. We thank Anja Ronnenberg and Sina Bode for excellent technical assistance.

DISCLOSURE

H Ehrenreich has submitted/holds user patents for EPO in stroke, schizophrenia and MS.

REFERENCES

1. Compston A, Coles A. (2002) Multiple sclerosis. *Lancet* 359:1221–31.
2. Hauser SL, Oksenberg JR. (2006) The neurobiology of multiple sclerosis: genes, inflammation, and neurodegeneration. *Neuron.* 52:61–76.
3. Buck D, Hemmer B. (2011) Treatment of multiple sclerosis: current concepts and future perspectives. *J. Neurol.* 258:1747–62.
4. Bartels C, Spate K, Krampe H, Ehrenreich H. (2008) Recombinant human erythropoietin: novel strategies for neuroprotective/neuro-regenerative treatment of multiple sclerosis. *Ther. Adv. Neurol. Disord.* 1:193–206.
5. Agnello D, *et al.* (2002) Erythropoietin exerts an anti-inflammatory effect on the CNS in a model of experimental autoimmune encephalomyelitis. *Brain Res.* 952:128–34.
6. Brines ML, *et al.* (2000) Erythropoietin crosses the blood-brain barrier to protect against experimental brain injury. *Proc. Natl. Acad. Sci. U. S. A.* 97:10526–31.
7. Chen SJ, *et al.* (2010) Erythropoietin enhances endogenous haem oxygenase-1 and represses immune responses to ameliorate experimental autoimmune encephalomyelitis. *Clin. Exp. Immunol.* 162:210–23.
8. Diem R, *et al.* (2005) Combined therapy with methylprednisolone and erythropoietin in a model of multiple sclerosis. *Brain.* 128:375–85.
9. Kang SY, *et al.* (2009) Expression of erythropoietin in the spinal cord of lewis rats with experimental autoimmune encephalomyelitis. *J. Clin. Neurol.* 5:39–45.
10. Leist M, *et al.* (2004) Derivatives of erythropoietin that are tissue protective but not erythropoietic. *Science.* 305:239–42.
11. Li W, *et al.* (2004) Beneficial effect of erythropoietin on experimental allergic encephalomyelitis. *Ann. Neurol.* 56:767–77.
12. Sattler MB, *et al.* (2004) Neuroprotective effects and intracellular signaling pathways of erythropoietin in a rat model of multiple sclerosis. *Cell Death Differ.* 11 (Suppl. 2):S181–92.
13. Savino C, *et al.* (2006) Delayed administration of erythropoietin and its non-erythropoietic derivatives ameliorates chronic murine autoimmune encephalomyelitis. *J. Neuroimmunol.* 172:27–37.
14. Thorne M, Moore CS, Robertson GS. (2009) Lack of TIMP-1 increases severity of experimental autoimmune encephalomyelitis: effects of darbepoetin alfa on TIMP-1 null and wild-type mice. *J. Neuroimmunol.* 211:92–100.
15. Yuan R, *et al.* (2008) Erythropoietin: a potent inducer of peripheral immuno/inflammatory modulation in autoimmune EAE. *PLoS One.* 3:e1924.
16. Zhang J, *et al.* (2005) Erythropoietin treatment improves neurological functional recovery in EAE mice. *Brain Res.* 1034:34–9.
17. Sargin D, Friedrichs H, El-Kordi A, Ehrenreich H. (2010) Erythropoietin as neuroprotective and neuroregenerative treatment strategy: comprehensive overview of 12 years of preclinical and clinical research. *Best Pract. Res. Clin. Anaesthesiol.* 24:573–94.
18. Ehrenreich H, *et al.* (2007) Exploring recombinant human erythropoietin in chronic progressive multiple sclerosis. *Brain.* 130:2577–88.
19. Ehrenreich H, *et al.* (2004) Erythropoietin: a candidate compound for neuroprotection in schizophrenia. *Mol. Psychiatry.* 9:42–54.
20. Siren AL, Fasshauer T, Bartels C, Ehrenreich H. (2009) Therapeutic potential of erythropoietin and its structural or functional variants in the nervous system. *Neurotherapeutics.* 6:108–27.
21. Boretius S, Kasper L, Tammer R, Michaelis T, Frahm J. (2009) MRI of cellular layers in mouse brain in vivo. *Neuroimage.* 47:1252–60.
22. Vandesompele J, *et al.* (2002) Accurate normalization of real-time quantitative RT-PCR data by geometric averaging of multiple internal control genes. *Genome Biol* 3:RESEARCH0034.
23. Merkler D, *et al.* (2005) Multicontrast MRI of remyelination in the central nervous system. *NMR Biomed.* 18:395–403.
24. Carlton WW. (1967) Studies on the induction of hydrocephalus and spongy degeneration by cuprizone feeding and attempts to antidote the toxicity. *Life Sci.* 6:11–9.
25. Lindner M, Fokuhl J, Linsmeier F, Trebst C, Stangel M. (2009) Chronic toxic demyelination in the central nervous system leads to axonal damage despite remyelination. *Neurosci. Lett.* 453:120–5.
26. Matsushima GK, Morell P. (2001) The neurotoxicant, cuprizone, as a model to study demyelination and remyelination in the central nervous system. *Brain Pathol.* 11:107–16.
27. Song SK, *et al.* (2005) Demyelination increases radial diffusivity in corpus callosum of mouse brain. *Neuroimage.* 26:132–40.
28. Tsiperson V, Li X, Schwartz GJ, Raine CS, Shafit-Zagardo B. (2010) GAS6 enhances repair following cuprizone-induced demyelination. *PLoS One.* 5:e15748.
29. Sargin D, Hassouna I, Sperling S, Siren AL, Ehrenreich H. (2009) Uncoupling of neurodegeneration and gliosis in a murine model of juvenile cortical lesion. *Glia.* 57:693–702.
30. Jung KH, *et al.* (2011) Molecular alterations underlying epileptogenesis after prolonged febrile seizure and modulation by erythropoietin. *Epilepsia.* 52:541–50.
31. Yatsiv I, *et al.* (2005) Erythropoietin is neuroprotective, improves functional recovery, and reduces neuronal apoptosis and inflammation in a rodent model of experimental closed head injury. *FASEB J.* 19:1701–3.
32. Villa P, *et al.* (2003) Erythropoietin selectively attenuates cytokine production and inflammation in cerebral ischemia by targeting neuronal apoptosis. *J. Exp. Med.* 198:971–5.
33. Iwai M, *et al.* (2010) Enhanced oligodendrogenesis and recovery of neurological function by erythropoietin after neonatal hypoxic/ischemic brain injury. *Stroke.* 41:1032–7.
34. Wergeland S, *et al.* (2011) Dietary vitamin D3 supplements reduce demyelination in the cuprizone model. *PLoS One.* 6:e26262.
35. Ji Y, Kutner A, Verstuyf A, Verlinden L, Studzinski GP. (2002) Derivatives of vitamins D2 and D3 activate three MAPK pathways and upregulate pRb expression in differentiating HL60 cells. *Cell Cycle.* 1:410–5.
36. Dusso AS, Puche RC. (1985) The effect of 1 alpha, 25-dihydroxycholecalciferol on iron metabolism. *Blut.* 51:103–8.
37. Skliar MI, *et al.* (1980) Effect of 1,25-dihydroxycholecalciferol and 1,25-dihydroxycholecalciferol glycoside on 2,3-diphosphoglycerate levels of the rat erythrocyte. *Pflugers Arch.* 389:81–3.
38. Liebetanz D, Merkler D. (2006) Effects of commissural de- and remyelination on motor skill behaviour in the cuprizone mouse model of multiple sclerosis. *Exp. Neurol.* 202:217–24.
39. Kipp M, Clarner T, Dang J, Copray S, Beyer C.

(2009) The cuprizone animal model: new insights into an old story. *Acta Neuropathol.* 118:723–36.
40. Liu L, *et al.* (2010) CXCR2-positive neutrophils are essential for cuprizone-induced demyelination: relevance to multiple sclerosis. *Nat. Neurosci.* 13:319–26.
41. Chen G, *et al.* (2007) Inhibitory effect on cerebral inflammatory agents that accompany traumatic brain injury in a rat model: a potential neuroprotective mechanism of recombinant human erythropoietin (rhEPO). *Neurosci. Lett.* 425:177–82.
42. Mausberg AK, *et al.* (2011) Erythropoietin ameliorates rat experimental autoimmune neuritis by inducing transforming growth factor-beta in macrophages. *PLoS One.* 6:e26280.
43. Sun Y, Calvert JW, Zhang JH. (2005) Neonatal hypoxia/ischemia is associated with decreased inflammatory mediators after erythropoietin administration. *Stroke.* 36:1672–8.
44. Mason JL, Suzuki K, Chaplin DD, Matsushima GK. (2001) Interleukin-1beta promotes repair of the CNS. *J. Neurosci.* 21:7046–52.
45. Gudi V, *et al.* (2011) Spatial and temporal profiles of growth factor expression during CNS demyelination reveal the dynamics of repair priming. *PLoS One.* 6:e22623.
46. Voss EV, *et al.* (2012) Characterisation of microglia during de- and remyelination: can they create a repair promoting environment? *Neurobiol. Dis.* 45:519–28.
47. Schmid CD, *et al.* (2009) Differential gene expression in LPS/IFNgamma activated microglia and macrophages: in vitro versus in vivo. *J. Neurochem.* 109 (Suppl. 1):117–25.